

Experimental study on fragmentation behaviors of molten LBE and water contact interface*

HUANG Wang-Li (黄望哩),^{1,2,3} SA Rong-Yuan (洒荣园),^{2,3,†} ZHOU Dan-Na (周丹娜),^{2,3}
JIANG Hua-Lei (姜华磊),^{2,3} and HUANG Qun-Ying (黄群英)^{2,3}

¹*University of Science and Technology of China, Hefei 230026, China*

²*Key Laboratory of Neutronics and Radiation Safety, Institute of Nuclear Energy Safety Technology,
Chinese Academy of Sciences, No. 350 Shushanhu Road, Hefei 230031, China*

³*Collaborative Innovation Center of Radiation Medicine of Jiangsu Higher Education Institution, Suzhou 215006, China*

(Received January 6, 2015; accepted in revised form March 6, 2015; published online December 20, 2015)

Based on the design of CLEAR (China LEad-based Reactor), it is important to study the molten LBE (Lead-Bismuth Eutectic)/water interaction following an incidental steam generator tube rupture (SGTR) accident. Experiments were carried out to investigate the fragmentation behavior of the molten LBE/water contacting interface, with a high-speed video camera to record the fragmentation behavior of 300–600 °C LBE at 20 °C and 80 °C of water temperature. Violent explosion phenomenon occurred at water temperature of 20 °C, while no explosion occurred at 80 °C. Shapes of the LBE debris became round at 80 °C of water temperature, whereas the debris was of the needle-like shape at 20 °C. For all the molten LBE and water temperatures in the present study, the debris sized at 2.8–5.0 mm had the largest mass fraction. The results indicate that the dominant physical mechanism of the molten LBE fragmentation was the Kelvin-Helmholtz instability between LBE/water direct contact interface.

Keywords: Steam generator tube rupture, Molten LBE, Fragmentation, Steam explosion, Interfacial instability

DOI: [10.13538/j.1001-8042/nst.26.060601](https://doi.org/10.13538/j.1001-8042/nst.26.060601)

I. INTRODUCTION

The Accelerator Driven System (ADS) was motivated by remarkable potentialities for transmutation of the long-lived nuclear wastes from the operation of nuclear power plants (NPPs) [1]. A project has been implemented to develop the ADS technology in China. Based on experiences of designing fusion reactor and the successful design and development of a series of PbLi test facilities, named DRAGON series, the FDS team has undertaken the ADS project, and proposed and developed the concept of China LEad-based Reactor (CLEAR). Lead-bismuth eutectic (LBE), due to its good thermal-physical and chemical properties, was chosen as the spallation target and primary coolant materials [2]. And LBE test facilities, named KYLIN loops, have been built-up to explore related technologies such as the compatibility with structural materials, thermal-hydraulic and safety characters [3–15].

In order to extract thermal power from the main vessel, steam generator unit (SGU) of CLEAR are placed inside the reactor vessel and immersing into the primary coolant (LBE). Housed in the SGU of harsh working conditions (i.e. high-temperature, high-pressure, corrosion etc.), the secondary water loop and the large number of pipes should be investigated on the impact of a steam generator tube rupture (SGTR) accident in the design and safety studies. In this postulated accident, highly pressurized water blasts into the low-pressure primary coolant, forming a thermal coolant-coolant interaction (CCI), similar to a fuel-coolant interaction (FCI) during

a sever NPP accident, which triggers various transients and evokes structure risks, causing escalation of the accident. A CCI with a sudden vaporization of the discharged water can initiate a sloshing motion of the heavy primary coolant, inducing strong impact pressures which may challenge the vessel integrity. A severe pressure build-up can also lead to a radial core compaction processes [16]. So, it is of significance to investigate the SGTR accident in the design and construction of China LEad-based Research Reactor (CLEAR-I), and to explore the protection and mitigation measures against the accident. In order to better understand the SGTR accident, the fragmentation procedure of the molten LBE when it contacts water should be studied because it may form a large-scale accident. The study can help disclose the local heat transfer behavior in micro interaction between the two liquids.

The interaction of molten lead-alloy with water has been investigated in different experiments. Flory *et al.* [17] reported the direct contact interaction of lead with water to support the hypothesis of surface instability as a mechanism. It was observed that outward burst occurred for the lead droplet at 500 °C. Furuya *et al.* [18] investigated the trigger mechanisms of vapor explosions by impinged water droplet on lead-bismuth and lead, the vapor explosion phenomenon was not observed when a water droplet was dropped into the molten lead and lead-alloy. Sa *et al.* [19, 20] poured small-scaled molten lead-alloy droplets into subcooled water and found that the peak pressure in fragmentation of LBE droplet increased with the droplet temperature, but no difference was observed with increasing temperature of the water subcooling. Li *et al.* [21, 22] obtained particles size distribution in water of LBE fragmentation at lower molten temperatures. Park *et al.* [23] and Sibamoto *et al.* [24] applied high-frame-rate neutron radiography technique to observe the penetration and boiling behavior of a plunging water jet in a molten LBE liquid pool. Ciampichetti *et al.* [1, 25] injected water into

* Supported by National Natural Science Foundation of China (No. 11302224) and Strategic Priority Science & Technology Program of the Chinese Academy of Sciences (No. XDA03040000)

† Corresponding author, rongyuan.sa@fds.org.cn

LBE to simulate the SGTR accident in LIFUS 5 facility, and fast system pressurization was detected. On the other hand, using SIMMER-III code, Wang *et al.* [16] evaluated a postulated SGTR accident in a lead cooled accelerator driven system.

However, the molten LBE and water interaction was rarely studied in median-scaled experiment. The interfacial behavior of LBE/water direct contact should be investigated in details to understand mechanisms of the rapid violent boiling, and the consequent accident. In the present study, thermal-hydraulic behavior of molten LBE/water interface was visually observed with a high-speed video camera at different temperatures of LBE and water. The visual information was analyzed to determine the fragmentation behavior and steam explosion behavior, etc. The results were compared with existing theories, and it was found that the Kelvin-Helmholtz instability could be the most probable reason of molten LBE/water interface breakup.

II. EXPERIMENT

A. Experimental Apparatus

Figure 1 shows schematically the experimental apparatus consisting mainly of an electric furnace, a crucible and a water tank. The crucible, made of stainless steel, is located inside the furnace of $\phi 190\text{ mm} \times 90\text{ mm}$. LBE was melted in the crucible with an electric heater. At the crucible bottom there is a nozzle with its opening being plugged by a conical-shaped rod, which is raised by a stepping motor actuator at the time of melt delivery. Ar gas is supplied via a regulator, so as to protect the molten LBE from oxidation. The water tank, of $\phi 250\text{ mm} \times 800\text{ mm}$, is composed of stainless steel, with quartz glass window to observe behavior of molten LBE/water interaction using the camera. A plate at the tank bottom is used to collect the posttest debris productions.

B. Instrumentation

The cylindrical radiant heater furnace (1 kW rating) was used to heat molten LBE. The temperature was monitored by a sheathed K-type thermocouple on top cover of the crucible. A 4 kW immersion electric heater was used to heat the water whenever needed, with a thermocouple sensor to control the water temperature. A high-speed video camera was installed to record video images of the molten LBE breakup process in 5740 frames per second.

C. Experimental procedure and test conditions

When the furnace and water tank were heated to a desired temperature set, the stepping motor raised the plug to open nozzle and inject the melt jet into the water. The fragmentation and breakup behavior of the molten LBE in water was observed by the video camera. After the test, water was drained

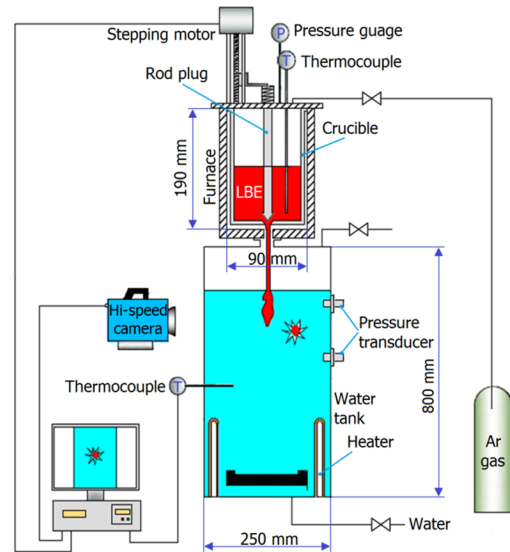


Fig. 1. (Color online) Schematic diagram of experimental apparatus.

from the tank and the debris was collected and dried. Particle size distribution of the fragmented debris was obtained by mechanical sieving of debris using a stack of sieves of 0.5–10 mm. The inventory of poured metal was about 450 g. The molten LBE temperatures were 300, 400, 500 and 600 °C. The water temperatures were 20–80 °C, i.e. from room temperature to the temperature related to design specifications of CLEAR-I, which is to be operated at 230 °C and 4 MPa, being equivalent of the water subcooling temperature of 80 °C in normal atmosphere. The nozzle diameter was 300 mm, the initial jet velocity was 2.42 m/s, and the free fall distance from the nozzle to the water surface was 5 mm. All the experiments were performed in atmosphere.

III. RESULTS AND DISCUSSION

Temperature effects on melt fragmentation were studied with LBE of 300, 400, 500 and 600 °C, at water temperature of 20 °C and 80 °C. Figure 2 shows the fragmentation behaviors, solidified fragments and distribution of debris sizes at water temperature of 20 °C.

In Fig. 2(a), extensive explosion was observed at 400, 500 and 600 °C. Take the 400 °C LBE case as an example, instability can be seen clearly at the melt side at 3.484 ms, and a slight expansion and explosion can be observed from the melt front and extended upward at 6.968 ms. With the center column of molten LBE decreased and disappeared, violent explosion occurred at 14.634 ms. This is because when molten LBE of higher temperatures was injected into the water, the steam produced in the contact interface was immediately broken up due to the 20 °C water. This induced disturbances of the contact interface, leading to further contact of molten LBE with more unstable steam and, finally, the vapor explosion. Also, molten LBE of higher temperatures, due to its lower viscosity and surface tension, is easier to break up into

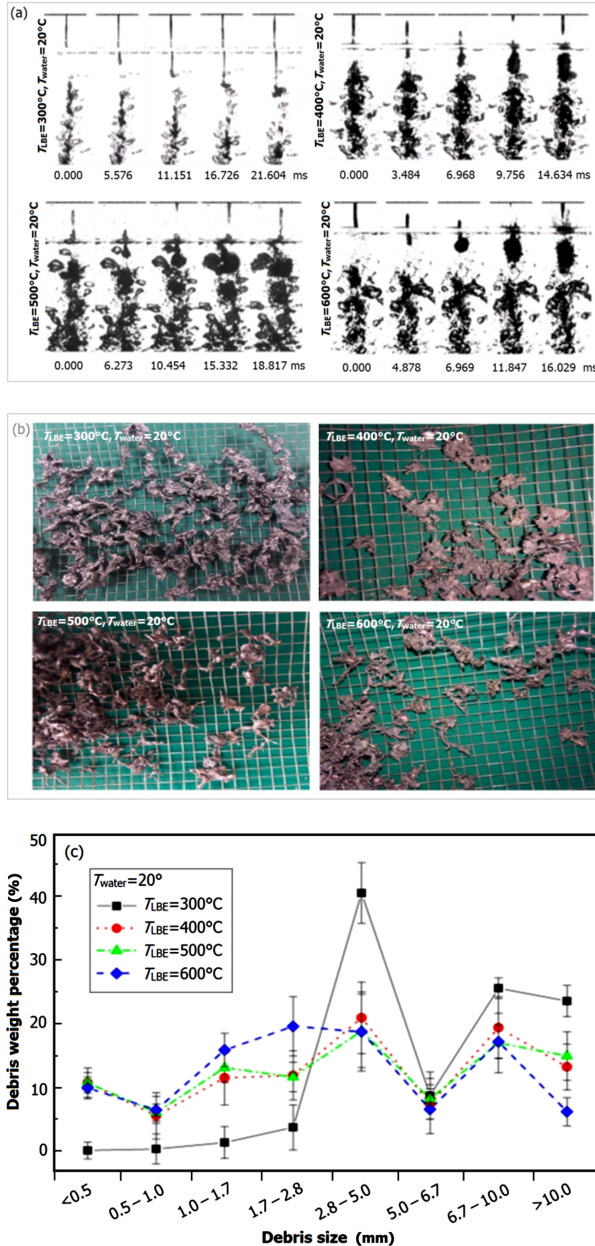


Fig. 2. (Color online) Fragmentation behaviors (a), debris shape (b) and size distribution (c) for 300–600 °C molten LBE at $T_{\text{water}} = 20^\circ\text{C}$.

fine particles in the coupling interaction of hydrodynamics and unstable disturbances.

However, no explosion was observed throughout the whole course at 300 °C.

The debris shown in Fig. 2(b) is in shapes of flakes and needles for LBE at 400, 500 and 600 °C, while they are in long strip and helix shapes for LBE at 300 °C, because internal energy of 300 °C molten LBE is too low to produce unstable steam in the contact interface, so the unstable disturbances induced by collapse of vapor film is very small. Besides, the shear force produced by the relative velocity of 300 °C melt and water was lower than the viscosity and surface tension of

the molten LBE, and only deformation behavior occurred in the surface of molten LBE jet by the shear force in the process of interaction. Thus, the debris is in long strip and helix shapes.

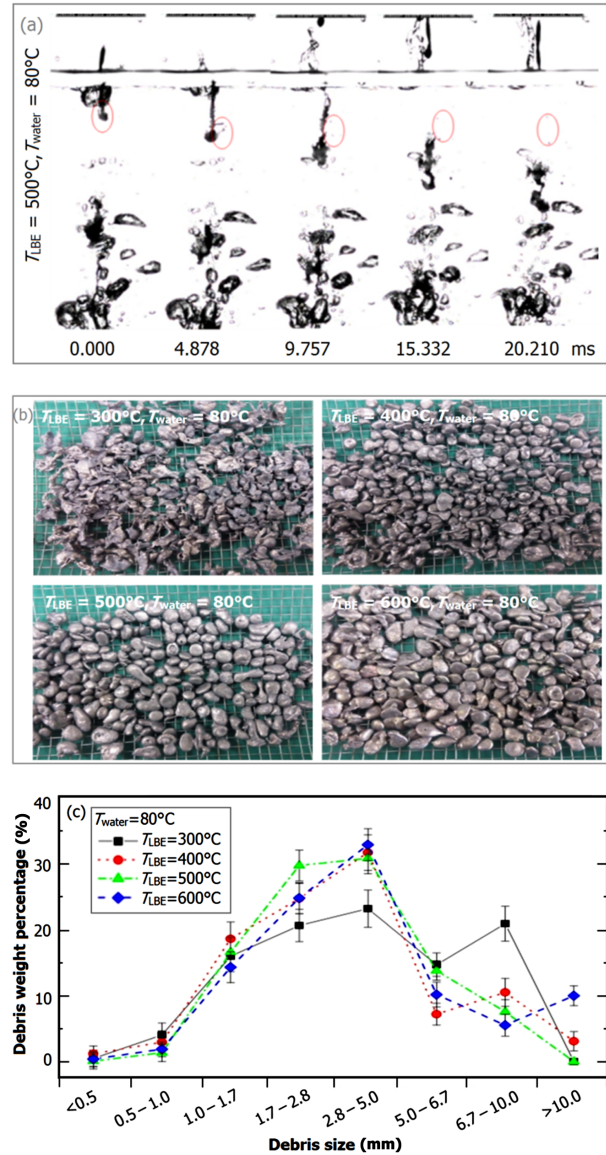


Fig. 3. (Color online) Fragmentation behaviors (a), debris shape (b) and size distribution (c) for 300–600 °C molten LBE at $T_{\text{water}} = 80^\circ\text{C}$.

Figure 2(c) shows debris size distributions for LBE temperatures of 300, 400, 500 and 600 °C at 20 °C of water temperature. The largest mass fraction of the debris almost lies in the size range of 2.8–5.0 mm. In the size range of 0.5–2.8 mm, the mass fraction increased with the molten LBE temperature. However, the largest mass fraction of the debris for 300 °C LBE was higher than other LBE temperatures, because no significant fragmentation occurred and the debris was mostly in long strip and spiral shapes sizes at about 3 mm.

At 80 °C of water temperature, no explosion could be observed, too. Figure 3(a) shows the typical fragmentation be-

haviors of 500 °C molten LBE at 80 °C. The areas enclosed by the circle express the fragmentation process of molten LBE, and some spherical fragments stripped from the leading edge of molten LBE can be seen roughly. The reason is that a stable vapor film could be easily formed in the leading edge in high temperature water, which lowers the latent heat of vaporization of water when the molten LBE contacts with water, and this decreases the ability of heat transfer and hinders the further contact of molten LBE and water.

The fragments were shown in Fig. 3(b). In general, the fragments were round, with smooth surface in all cases, and the debris shapes at different LBE temperatures did change significantly. In Fig. 3(c), the largest mass fraction of the debris was still in the size range of 2.8–5.0 mm, which was similar to the water temperature 20 °C, and the debris sizes corresponding to the largest mass fraction at different LBE temperatures did not change significantly.

The debris at each water temperature, shown in Figs. 2(b) and 3(b), differs significantly from each other. At 20 °C, the debris was generally of fluffy needles and flakes, due to violent explosions when molten LBE was plunged into water; whereas at 80 °C the debris has round and smooth surface generally, owing to the presence of stable vapor films formed in the fragmentation, in which the fragmented particles were entrained and solidified inside the vapor films.

Comparing the distributions of debris weight percentages at water temperature of 20 °C and 80 °C (Figs. 2(c) and 3(c)), the debris size of the highest mass fraction can be considered as the most probable debris size in molten alloy jet breakup, and as the results of dominant jet breakup mechanisms [23]. The largest mass fraction lied in the size range of 2.8–5.0 mm, with the largest mass fraction of about 40% and 20% for 20 °C and 80 °C, respectively.

IV. THEORETICAL COMPARISON OF THE EXPERIMENTAL RESULTS

It is well-known that the fragmentation is related to the wavelength of unstable interface. Several theories have been proposed for fragmentation of molten alloys, such as the Rayleigh-Taylor instability, Kelvin-Helmholtz instability, Critical Weber number criteria and Instability of surface wave on gas-liquid interface [27]. By the Rayleigh-Taylor instability, the fragmentation of a cylindrical jet is caused at the jet leading edge due to acceleration in the normal direction to the melt-water interface, while by the Kelvin-Helmholtz instability it is at the jet surface due to the relative velocity of melt and water in the direction parallel with the interface [26].

The wave length of the fastest growth rate, λ_1 , is expressed by Eq. (1) based on the Rayleigh-Taylor instability [28]:

$$\lambda_1 = 2\pi\{3\sigma/[(\rho_j - \rho_w)g]\}^{1/2}, \quad (1)$$

where, σ is surface tension; ρ_j and ρ_w are density of jet and density of water, respectively; and g is acceleration. Using physical properties of molten LBE, we have $\lambda_1 = 23$ mm, which is far greater than the most probable fragment size of 2.8–5.0 mm.

In the Kelvin-Helmholtz instability on the interface parallel to the direction of gravity, a critical relative velocity, U , above which some initial disturbances of large wavelength are unstable is given by [29]

$$U = [2\pi\sigma(\rho_j - \rho_w)/(\lambda\rho_j\rho_w)g]^{1/2}. \quad (2)$$

Given the relative velocity, the minimum unstable wavelength, λ_2 , can be obtained by

$$\lambda_2 = 2\pi\sigma(\rho_j - \rho_w)/(U^2\rho_j\rho_w). \quad (3)$$

Using physical properties of molten LBE and the initial jet velocity, the minimum wavelength could be calculated. The results in Fig. 4 were calculated with Eqs. (1) and (3) by using the following physical properties of the LBE: melting temperature, 125 °C; density, 10 380 kg/cm³; specific heat, 148 J/(kg K); thermal conductivity, 9.65 W/(m K), and surface tension N/m. The symbol in Fig. 4 shows the most probable fragment size. Comparing the experimental data with the calculation results of the Kelvin-Helmholtz instability, the most probable experimental fragment size was in the range of 2.8–5.0 mm. Therefore, the Kelvin-Helmholtz instability is the dominant physical mechanism of the molten LBE fragmentation in the present experimental conditions.

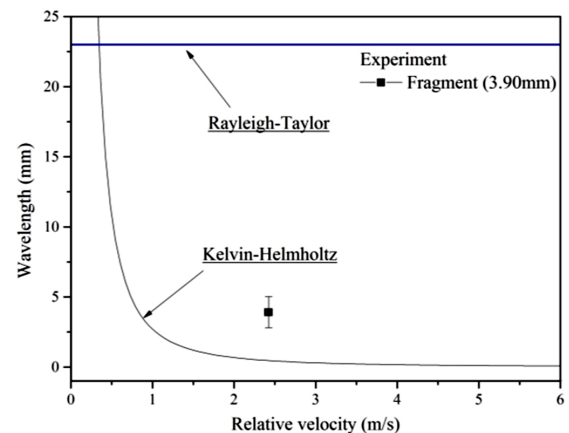


Fig. 4. (Color online) Unstable minimum wavelength in Kelvin-Helmholtz instability, Rayleigh-Taylor instability.

V. CONCLUSION

In order to investigate the fragmentation behavior of the molten LBE/water contacting interface, experiments were initiated by utilizing a visualization experimental facility with a high-speed video camera to observe the fragmentation behavior and the unstable wavelength on LBE/water interface, and the solidified fragments shape and mass fraction distribution were analysis after experiments. These data yielded the following results.

1) The visualization pictures present an obvious violent explosion phenomenon of LBE in water when water temperature is 20 °C, and no explosion occurred in water under 80 °C.

2) The shape of the LBE debris became round with the increasing water temperature and the shape of the debris was not change significantly with increasing molten LBE temperature. The debris size of the highest mass fraction was 2.8–5.0 mm, which was not influenced by water temperature and molten LBE temperature in the present study.

3) The dominant physical mechanism of the molten LBE fragmentation was Kelvin-Helmholtz instability be-

tween LBE/water contacting interface.

ACKNOWLEDGEMENT

The authors gratefully acknowledge FDS team supplying a good research environment all these years and other members of FDS team for their assistance.

-
- [1] Ciampichetti A, Pellini D, Agostini P, et al. Experimental and computational investigation of LBE–water interaction in LIFUS 5 facility. Nucl Eng Des, 2009, **239**: 2468–2478. DOI: [10.1016/j.nucengdes.2009.08.007](https://doi.org/10.1016/j.nucengdes.2009.08.007)
- [2] Sobolev V. Thermophysical properties of lead and lead-bismuth eutectic. J Nucl Mater, 2007, **362**: 235–247. DOI: [10.1016/j.jnucmat.2007.01.144](https://doi.org/10.1016/j.jnucmat.2007.01.144)
- [3] Wu Y C and FDS Team. Conceptual design activities of FDS series fusion power plants in China. Fusion Eng Des, 2006, **81**: 2713–2718. DOI: [10.1016/j.fusengdes.2006.07.068](https://doi.org/10.1016/j.fusengdes.2006.07.068)
- [4] Wu Y C, Qian J P and Yu J N. The fusion-driven hybrid system and its material selection. J Nucl Mater, 2002, **307–311**: 1629–1636. DOI: [10.1016/S0022-3115\(02\)01272-2](https://doi.org/10.1016/S0022-3115(02)01272-2)
- [5] Wu Y C and FDS Team. Conceptual design of the China fusion power plant FDS-II. Fusion Eng Des, 2008, **83**: 1683–1689. DOI: [10.1016/j.fusengdes.2008.06.048](https://doi.org/10.1016/j.fusengdes.2008.06.048)
- [6] Wu Y C, Huang Q Y, Zhu Z Q, et al. R&D of Dragon Series Lithium Lead loops for Material and Blanket Technology Testing. Fusion Sci Tech, 2012, **62**: 272–275.
- [7] Wu Y C and FDS Team. Conceptual design and testing strategy of a dual functional lithium-lead test blanket module in ITER and EAST. Nucl Fusion, 2007, **47**: 1533–1539. DOI: [10.1088/0029-5515/47/11/015](https://doi.org/10.1088/0029-5515/47/11/015)
- [8] Wu Y C and FDS Team. Fusion-based hydrogen production reactor and its material selection. J Nucl Mater, 2009, **386–388**: 122–126. DOI: [10.1016/j.jnucmat.2008.12.075](https://doi.org/10.1016/j.jnucmat.2008.12.075)
- [9] Qiu L J, Wu Y C, Xiao B J, et al. A low aspect ratio tokamak transmutation system. Nucl Fusion, 2000, **40**: 629–633.
- [10] Wu Y C, Jiang J Q, Wang M H, et al. A fusion-driven subcritical system concept based on viable technologies. Nucl Fusion, 2011, **51**: 103036. DOI: [10.1088/0029-5515/51/10/103036](https://doi.org/10.1088/0029-5515/51/10/103036)
- [11] Huang Q Y, Li C J, Li Y, et al. Progress in development of China low activation martensitic steel for fusion application. J Nucl Mater, 2007, **367–370**: 142–146. DOI: [10.1016/j.jnucmat.2007.03.153](https://doi.org/10.1016/j.jnucmat.2007.03.153)
- [12] Wu Y C, Bai Y Q, Song Y, et al. Conceptual design of China lead-based research reactor CLEAR-I. Chin J Nucl Sci Eng, 2014, **34**: 201–208. (in Chinese)
- [13] Wang Y Q, Huang Q Y, Wu B, et al. The performance of Pt/air oxygen sensors in stagnant Pb-Bi eutectic at high temperatures. Nucl Sci Tech, 2014, **25**: 060602. DOI: [10.13538/j.1001-8042/nst.25.060602](https://doi.org/10.13538/j.1001-8042/nst.25.060602)
- [14] Lu Y, He J, Zhu Z Q, et al. Preliminary calibration test and analysis of electromagnetic flow-meter in liquid lead-bismuth. Nucl Tech, 2014, **37**: 080603. (in Chinese) DOI: [10.11889/j.0253-3219.2014.hjs.37.080603](https://doi.org/10.11889/j.0253-3219.2014.hjs.37.080603)
- [15] Yao C M, Huang Q Y, Zhu Z Q, et al. Data acquisition and control system for lead-bismuth loop KYLIN-II-M. Nucl Sci Tech, 2015, **26**: 010401. DOI: [10.13538/j.1001-8042/nst.26.010401](https://doi.org/10.13538/j.1001-8042/nst.26.010401)
- [16] Wang S S, Flad M, Maschek W, et al. Evaluation of a steam generator tube rupture accident in an accelerator driven system with lead cooling. Prog Nucl Energ, 2008, **50**: 363–369. DOI: [10.1016/j.pnucene.2007.11.018](https://doi.org/10.1016/j.pnucene.2007.11.018)
- [17] Flory K, Paoli R and Mesler R. Molten metal-water explosion. Chem Eng Prog, 1969, **65**: 50–54.
- [18] Furuya M and Arai T. Effect of surface property of molten metal pools on triggering of vapor explosions in water droplet impingement. Inter J Heat and Mass Transfer, 2008, **51**: 4439–4446. DOI: [10.1016/j.ijheatmasstransfer.2008.02.025](https://doi.org/10.1016/j.ijheatmasstransfer.2008.02.025)
- [19] Sa R Y and Minoru T. Thermal interaction of lead-alloy droplet with subcooled water in pool water tank. J Energ Power Eng, 2011, **5/7**: 579–589.
- [20] Sa R Y, Takahashi M and Moriyama K. Study on fragmentation behavior of liquid lead alloy droplet in water. Prog Nucl Energ, 2011, **53**: 895–901. DOI: [10.1016/j.pnucene.2011.05.003](https://doi.org/10.1016/j.pnucene.2011.05.003)
- [21] Li H X, Luo Z X and Chen T K. Experimental investigation on the fragmentation behavior of high temperature molten melt drops. Chin J Eng Thermophys, 2003, **24**: 625–628. (in Chinese)
- [22] Li L X, Li H X and Chen T K. Experimental investigation on movement characteristics of molten melt drops in Coolant. Chin J Nucl Power Eng, 2007, **28**: 36–41. (in Chinese)
- [23] Park H, Shibamoto Y, Maruyama Y, et al. Visualization of plunging jet behavior in molten alloy. Proceedings of 7th International Conference on Nuclear Engineering (ICONE 7), Tokyo, Japan, 1999.
- [24] Shibamoto Y, Kukita Y and Nakamura H. Small-scale experiment on subcooled water jet injection into molten alloy by using fluid temperature-phase coupled measurement and visualization. J Nucl Sci Tech, 2007, **44**: 1059–1069. DOI: [10.1080/18811248.2007.9711347](https://doi.org/10.1080/18811248.2007.9711347)
- [25] Ciampichetti A, Bernardi D, Cadiou T, et al. LBE–water interaction in LIFUS 5 facility under different operating conditions. J Nucl Mater, 2011, **415**: 449–459. DOI: [10.1016/j.jnucmat.2011.04.051](https://doi.org/10.1016/j.jnucmat.2011.04.051)
- [26] Bang K H, Kim J M and Kim D H. Experimental study of melt jet breakup in water. J Nucl Sci Tech, 2003, **40**: 807–813. DOI: [10.1080/18811248.2003.9715422](https://doi.org/10.1080/18811248.2003.9715422)
- [27] Abe Y, Matsuo E, Arai T, et al. Fragmentation behavior during molten material and coolant interactions. Nucl Eng Des, 2006, **236**: 1668–1681. DOI: [10.1016/j.nucengdes.2006.04.008](https://doi.org/10.1016/j.nucengdes.2006.04.008)
- [28] Carey V P. Liquid-vapor phase-change phenomena. Hemisphere, 1992.
- [29] Magallon D, Huhtiniemi I and Hohmann H. Lessons learned from FARO/TERMOS corium melt quenching experiments. Proc. OECD/CSNI Specialists Meeting on Fuel-Coolant Interactions, JAERI-Conf 97-011, Japan Atomic Energy Research Institute, 1997, 431–446.